JOURNAL OF BACTERIOLOGY, Mar. 1997, p. 1628–1635 Vol. 179, No. 5
0021-9193/97/$04.00+0

Relationship of *Treponema denticola* Periplasmic Flagella to Irregular Cell Morphology

JOHN D. RUBY,[1] HONG LI,[2] HOWARD KURAMITSU,[2] STEVEN J. NORRIS,[3] STUART F. GOLDSTEIN,[4] KAROLYN F. BUTTLE,[5] AND NYLES W. CHARON[1]*

Department of Microbiology and Immunology, Robert C. Byrd Health Sciences Center, West Virginia University, Morgantown, West Virginia 26506-9177[1]; Department of Oral Biology, State University of New York at Buffalo, Buffalo, New York 14214[2]; Department of Pathology and Laboratory Medicine, Medical School, University of Texas Health Sciences Center at Houston, Houston, Texas 77225[3]; Department of Genetics and Cell Biology, University of Minnesota, St. Paul, Minnesota 55108[4]; and Biological Microscopy and Image Reconstruction Resource, NIH Biotechnological Resource, Wadsworth Center for Laboratories and Research, New York State Department of Health, Albany, New York 12201-0509[5]

Received 7 June 1996/Accepted 26 December 1996

Treponema denticola **is an anaerobic, motile, oral spirochete associated with periodontal disease. We found that the periplasmic flagella (PFs), which are located between the outer membrane sheath and cell cylinder, influence its morphology in a unique manner. In addition, the protein composition of the PFs was found to be quite complex and similar to those of other spirochetes. Dark-field microscopy revealed that most wild-type cells had an irregular twisted morphology, with both planar and helical regions, and a minority of cells had a regular right-handed helical shape. High-voltage electron microscopy indicated that the PFs, especially in those regions of the cell which were planar, wrapped around the cell body axis in a right-handed sense. In those regions of the cell which were helical or irregular, the PFs tended to lie along the cell axis. The PFs caused the cell to form the irregular shape, as two nonmotile, PF-deficient mutants (JR1 and HL51) were no longer irregular but were right-handed helices. JR1 was isolated as a spontaneously occurring nonmotile mutant, and HL51 was isolated as a site-directed mutant in the flagellar hook gene *flgE*. Consistent with these results is the finding that wild-type cells with their outer membrane sheath removed were also right-handed helices similar in shape to JR1 and HL51. Purified PFs were analyzed by two-dimensional gel electrophoresis, and several protein species were identified. Western blot analysis using antisera to *Treponema pallidum* PF proteins along with N-terminal amino acid sequence analysis indicated *T. denticola* PFs are composed of one class A sheath protein of 38 kDa (FlaA) and three class B proteins of 35 kDa (FlaB1 and FlaB2) and one of 34 kDa (FlaB3). The N-terminal amino acid sequences of the FlaA and FlaB proteins of *T. denticola* were most similar to those of *T. pallidum* and *Treponema phagedenis*. Because these proteins were present in markedly reduced amounts or were absent in HL51, PF synthesis is likely to be regulated in a hierarchy similar to that found for flagellar synthesis in other bacteria.**

Spirochetes are recognized for their unique cell morphology and unusual means of motility (5, 48). In most spirochetes, the primary structural component of the cell body is a flexible yet semirigid helically shaped cell cylinder (5). *Borrelia burgdorferi* is an exception, since it has a rod-shaped cell cylinder (13, 15). Helical periplasmic flagella (PFs) are closely associated with the spirochetal protoplasmic cell cylinder (PC) and are embedded in the cytoplasmic membrane and cell wall near each end of the cell (5, 6, 17); each PF is inserted at only one end. Surrounding the entire cell is an outer membrane sheath (OS) (5). Genetic evidence indicates that the PFs are essential for the motility of several spirochete species (4, 8, 26, 28, 37, 44). The PFs vary in number, length, and protein composition among the spirochete species. Depending on the species, the PFs may or may not overlap in the center of the cell (5, 8). PFs from most spirochete species are composed of a sheath made up of one to two class A proteins and a core composed of at least two different class B proteins (3, 8, 23, 35).

Recent evidence suggests that spirochete morphology is markedly influenced by complex interactions between the PFs and cell cylinders. This conclusion is drawn from an analysis of mutants which are either devoid of or have altered PFs derived from several spirochete species, including *Leptonema* (formerly *Leptospira*) *illini* (19), *Treponema phagedenis*, and *B. burgdorferi*. In both *L. illini* and *T. phagedenis*, the PFs are short, do not overlap in the center of the cell, and influence the shape of the cell at the ends in the domain where they reside. The PFs of *L. illini* cause the helically shaped cell cylinder to form either hook- or spiral-shaped ends (1, 4, 14). In *T. phagedenis*, the left-handed PFs cause the end of the cell to be bent or be left-handed, with a larger helical pitch and diameter than the PFs (7). The PFs overlap in the center of the cell in *B. burgdorferi* (20) and cause the entire cell to take on a flat-wave morphology (13, 15).

Very little is known about the morphology of the oral spirochete *Treponema denticola*, which is implicated in periodontal diseases (30, 45). Several potential virulence factors, including motility, are associated with these organisms (11). Compared to other spirochetes, *T. denticola* cells are relatively small (0.12 to 0.25 μm in diameter and 6 to 16 μm long) (5, 46). They have two PFs inserted subterminally at each end, and the PFs overlap in the center of the cell (5, 46). Conflicting reports in the literature concern their overall morphology. Cox reported that *T. denticola* has a flat-wave morphology (10), whereas Socransky et al. (46) indicated that the morphology of *T. denticola* was

* Corresponding author. Mailing address: Department of Microbiology and Immunology, West Virginia University, Box 9177, Robert C. Byrd Health Sciences Center, Morgantown, WV 26506-9177. Phone: (304) 293-4170. Fax: (304) 293-7823. E-mail: ncharon@wvu.edu.

variable, with loosely coiled, tightly coiled, and irregularly coiled cells being present. Here, we present evidence from dark-field microscopy that indicates that most cells of *T. denticola* have a highly irregular morphology that is neither helical nor a flat planar wave. Moreover, high-voltage electron microscopy indicated that the PFs interact with the PC in a very complicated manner. We made use of both site-directed (26) and spontaneous mutants to determine the role of the PFs in generating these morphological characteristics. These studies, along with those of Rosey et al. on *Serpulina hyodysenteriae* (41), are among the first to exploit site-directed mutagenesis to analyze spirochete morphology and motility. We also analyzed the chemical composition of the PFs of *T. denticola* and compared them to those of other spirochetes. We present evidence that the PFs are comprised of one FlaA and three FlaB proteins. These proteins are most similar to those of *Treponema pallidum* and *T. phagedenis*, based on N-terminal amino acid sequences, and are present in reduced amounts in both PF mutants.

MATERIALS AND METHODS

Bacterial strains and culture conditions. *T. denticola* ATCC 33520 and 35405 were obtained from the American Type Culture Collection, Rockville, Md. Cells were grown in NOS medium (25) without glucose, and colony isolation was achieved by pipetting 1 ml of cell dilutions in NOS medium onto 0.5% Noble agar plates (Difco Laboratories, Detroit, Mich.) that were prereduced in an anaerobic chamber for several days. Alternatively, colonies were obtained from pour plates as previously described (26). Cultures were incubated at 35°C in a Coy anaerobic chamber with an internal atmosphere of 80% nitrogen–10% carbon dioxide–10% hydrogen (28). Cell densities were determined by using a nephelometer, with readings correlated to direct cell counts (7, 43).

Isolation of motility mutants and revertant. Two different mutants were used in the study. A wild-type clone of *T. denticola* 33520, which was previously selected for maximum colony diameter (6 mm after 10 days of incubation), was grown in broth to late logarithmic phase and spread onto agar plates. Plates were incubated for 10 days, and small colonies (<1-mm diameter) were picked and inoculated into NOS broth. After 48 h, the cultures were screened for motility by dark-field microscopy. One of approximately 20 clones was nonmotile (mutant JR1). A spontaneously occurring revertant to motility (JR1-r) was obtained by a method similar to that described for *T. phagedenis* (28). JR1 cells were inoculated into the center of swarm plates containing NOS medium plus 0.3% agarose and incubated for 2 weeks. The outer edge of the swarm was picked, the cells were subcloned, and the clones were screened for motility by dark-field microscopy. A second nonmotile mutant, HL51, has been previously described (26). This mutant was obtained from *T. denticola* 35405, and it contains a tandem erythromycin-resistant cassette inserted within the PF hook gene *flgE*. Electron microscopy had previously shown that this mutant contained no detectable PFs (26).

Dark-field photomicroscopy. Late-logarithmic-phase cells were analyzed by using a Leitz microscope, a 54× or 100× objective, and dark-field illumination as previously described (7). PCs free of the OS were obtained by incubation in 1.0% Triton X-100 in H_2O for 1 h at 37°C. Helical handedness (left or right), pitch, and diameter were determined as previously described (7). In certain experiments, glutaraldehyde was added to a final concentration of 1%. To assay for translational motility, methylcellulose (2% [wt/vol]; 4,000 mesh; Fisher) was added to NOS medium without rabbit serum and incubated anaerobically overnight. Cells were observed by dark-field microscopy by mixing an equal volume of washed cells and NOS medium containing methylcellulose. Viscosity was measured with a Brookfield DV III rheometer (Brookfield Engineering, Stroughton, Mass.).

Electron microscopy. Routine ultrastructural observations of negatively stained cells were made with a JEOL 100CX or a Philips 300 microscope. One milliliter of a late-logarithmic-phase culture was centrifuged at 14,000 × *g* for 90 s at room temperature, and the pellet was washed twice in cold H_2O. A drop of the cell suspension was placed on Parafilm, and a carbon-coated Formvar grid was floated on the drop for 30 s. The preparation was then stained with 2% uranyl acetate for 10 s. Purified PFs were also stained by using this procedure. Alternatively, to visualize PFs attached to cells, the OS was removed by resuspending washed cells in 1% Triton X-100 for 1 h at 37°C and washed with H_2O as described above. The cell suspension was placed on a grid for 1 min and stained with 1% phosphotungstate for 2 min. *T. denticola* cells were also fixed and embedded according to standard protocols, and thin sections were prepared for viewing under the electron microscope (21). The preparation and analysis of thick sections for high-voltage electron microscopy was done as previously described for *L. illini* (13).

Isolation of PFs. The method used to purify PFs combined techniques used by Cockayne et al. (9) and Limberger and Charon (28). One liter of late-logarithmic-phase cells (2×10^9 cells/ml) was centrifuged at 12,000 × *g* for 10 min at 5°C, and the pellet was resuspended in 100 ml of cold 67 mM phosphate-buffered saline, pH 7.4. The cells were washed twice with cold phosphate-buffered saline by centrifugation, and the final pellet was resuspended in 90 ml of cold 100 mM Tris buffer, pH 8.0 (T buffer). Ten milliliters of 10% Triton X-100 was slowly added, and the mixture was incubated for 1 h at 37°C. The cell suspension was centrifuged at 12,000 × *g* for 10 min at 5°C and resuspended in 100 ml of T buffer. Centrifugation was repeated, and the final pellet was suspended in 80 ml of cold T buffer. PFs were sheared from the cells by using a vortex mixer with 1 mm glass beads. Specifically, the contents of a 50-ml glass tube one-third filled with glass beads and 5 ml of the cell suspension were mixed for 30 s. After all 80 ml of cell suspension was treated, the suspension was centrifuged at 18,000 × *g* for 30 min at 5°C, and the supernatant fluid containing the sheared PFs was removed, pooled, and centrifuged at 100,000 × *g* for 1 h at 5°C in 0.2% Triton X-100. The pellet was collected, layered on a 10 to 66% Hypaque gradient, and centrifuged at 100,000 × *g* for 2 h at 5°C. The band containing the PFs was removed with an 18-gauge needle and dialyzed overnight at 4°C in 1.5 liter of 10 mM Tris–5 mM EDTA (pH 8.0) with 0.05% azide. The PFs were collected and stored at 4°C.

Gel electrophoresis, Western blotting, and protein sequencing. Sodium dodecyl sulfate-polyacrylamide gel electrophoresis (SDS-PAGE) and Western blotting were carried out as previously described (49). The resolving gels contained 10% acrylamide and were stained with Coomassie blue R. Two-dimensional gel electrophoresis and Western blotting were carried out as described by Norris et al. (34) except that polyvinyl difluoride (PVDF) membranes (Millipore Corp., Bedford, Mass.) were used in Western blot analysis (32). Blots were developed by using horseradish peroxidase second antibody with either 4-chloronaphthol or the ECL luminol assay of Amersham. Approximately 14 μg of PFs or 10^8 cells were used in each analysis. The antisera directed to the *T. pallidum* 37-kDa FlaA protein, 33-kDa FlaB2 protein, and 33- to 34-kDa *T. phagedenis* FlaB proteins have been previously described (28, 29, 34). N-terminal amino acid sequence determination was performed on spots corresponding to each of the major PF proteins following two-dimensional electrophoresis, transfer to PVDF membranes, and visualization of spots by Coomassie blue R staining (34). Sequence analysis was performed directly from PVDF membrane fragments by Richard G. Cook of the Baylor College of Medicine, using a model 477A sequenator (Applied Biosystems, Foster City, Calif.).

RESULTS

Cell morphology and motility of wild-type cells in broth and methylcellulose. Dark-field microscopy was used to analyze the morphology of exponentially growing *T. denticola* 33520 and 35405. Greater than 85% of exponential-phase cells in broth culture or in methylcellulose (1.6%, centipoise = 85 at 25°C) had an irregular (twisted) morphology along their entire lengths (Fig. 1a), with the minority of cells having a right-handed helical configuration (Table 1). Focusing on different planes of these irregular cells indicated that they contain both planar and helical regions, but it was difficult to distinguish a distinct pattern. These morphological forms were distinguished only by using high-magnification (≥×540) microscopy. To determine if the two morphological forms were the result of a genetically mixed population, several low (<5)-passage subclones of each strain were analyzed. All subclones yielded approximately the same proportion of irregularly versus helically shaped cells as the original culture. In addition, cells often grew in chains, and we occasionally observed chains in which both morphological forms were present. These results indicate that the different morphological forms are the result of phenotypic variation. The irregular and helical morphological forms were relatively stable when cells were tracked for several minutes, and only rarely did one form convert to the other. Although both forms were actively motile in broth but were incapable of translation in a given direction (i.e., the cells showed movement but no displacement), both forms translated in a gel-like medium containing 1% methylcellulose. These results are similar to those reported by others, which indicate that *T. denticola* translates only in a highly viscous gel-like medium (22, 40). No cells with a completely planar waveform were detected. Cells with a rod-shaped appearance for part of the cell length were occasionally detected, as were cells with protruding helical PFs (6).

Several parameters were examined to determine the factors

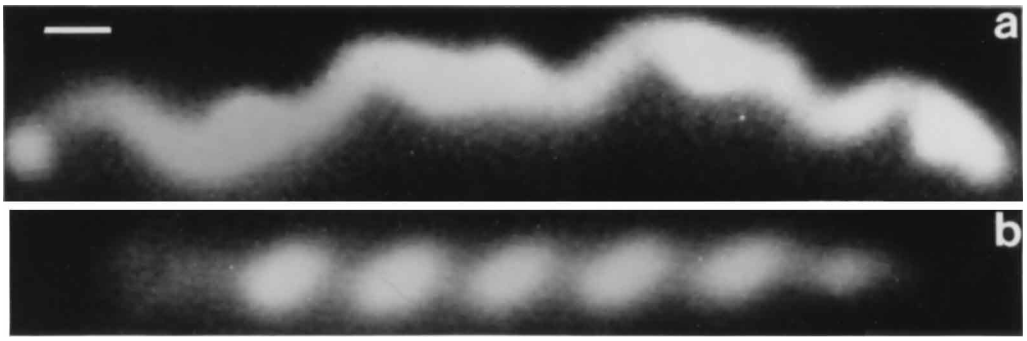

FIG. 1. (a) Wild-type *T. denticola* of strain 35405 exhibiting the typical irregular morphology. *T. denticola* 33520 was indistinguishable from strain 35405. (b) Mutant HL51 exhibiting a right-handed helical morphology. The plane of focus was below the cell. Mutant JR1 was indistinguishable from HL51. Bar, 1.0 μm. Tilt angle = ±5%.

that influence cell shape. Glutaraldehyde treatment did not change cell morphology. Cells of strain 33520 were obtained with the OS removed were obtained by using Triton X-100. Electron microscopy using both thin sectioning and negative staining confirmed that these stripped cells had their OS removed and that the PFs were no longer closely associated with the cell body (42, 43). Dark-field microscopy revealed that the isolated PCs were no longer irregular in shape; cells were converted to a right-handed helical form with a helical pitch and diameter slightly smaller than those of the helical wild-type cells (Table 1). Evidently, the OS in part influences cell shape, as removal of this structure causes the cells to lose their irregular morphology.

High-voltage analysis of wild-type cells. To analyze the relationship of the PFs to the PC, stereo pairs of thick sections of cells of strain 33520 were prepared by high-voltage electron microscopy (Fig. 2). The helix pitch (or wavelength of planar regions) of the cells was found to be 1.26 ± 0.16 μm (n = 20 cells), in good agreement with our measurements on light micrographs. The cell body diameter was 0.21 ± 0.01 μm (n = 23 cells). Regions along the PC could have a right-handed helical form (n = 9 cells) or a flat meandering waveform (n = 6 cells). They also had three-dimensional curves that gave them an irregular appearance.

The PFs formed a single bundle, which could be seen as a ridge running along its entire length in most cells. Within the bends of the PC, the ridge was always on the axial (inner) side of the PC (n = 28 cells). The ridge wound around the PC body helix in a right-handed sense (n = 17 cells). This winding was most pronounced when the PC had a flat waveform. Along the cell axis, the ridge formed a left-handed helix in those regions which had a flat waveform (n = 9 cells). When the PC appeared as right-handed or irregular, the diameter of the ridge helix was diminished. The helix diameter of the ridge helix could diminish enough to appear to lie along the cell axis (n = 6 cells).

Cell morphology and motility of PF motility mutants. Two PF-deficient mutants were analyzed with respect to cell morphology. JR1 was obtained as a spontaneously occurring nonmotile mutant of strain 33520. This mutant failed to swarm on agar plates and was completely nonmotile, as determined by dark-field microscopy. Electron microscopy indicated that JR1 was deficient in synthesizing full-length PFs. Whereas the wild type had two PFs inserted subterminally at each cell end that extended along the length of the cells (Fig. 3a), JR1 had short, stubby filaments 200 nm in length (Fig. 3b). Dark-field microscopy revealed that short protrusions occasionally occurred on JR1 and rotated at >10 Hz in a manner similar to the protrusions on wild-type cells (6, 42, 43).

Mutant HL51 was obtained by a directed insertional mutation of the *flgE* gene of strain 35405, and electron microscopy indicated that this mutant lacked PFs (26). No helical protrusions were detected in this mutant, a result consistent with previous observations that these protrusions are comprised of PFs surrounded by the OS (6). Dark-field microscopy revealed that both JR1 and HL51 cells had a right-handed helical morphology with a helical pitch and diameter identical to those of the wild-type helical cells (Fig. 1b; Table 1); no irregularly shaped cells were detected. A spontaneously occurring motile revertant of JR1 (JR1-r) was indistinguishable from the wild-type with respect to presence of PFs and irregular cell morphology. Taken together, these results indicate that the PFs are involved in the motility and the formation of the irregular morphology of *T. denticola.*

Structure and composition of purified PFs. The PFs of wild-type cells of strain 33520 were analyzed in detail. Electron microscopy revealed that the PFs were wave-like in appearance and were 23 nm in diameter for most of their length. One end often appeared tapered and was 18 nm in diameter. Similar results have been reported by others (18). As previously reported, purified PFs in 0.5% methylcellulose were left-handed, with a helical pitch of 0.78 μm and a helical diameter of 0.26 μm (Table 1) (6). Four polypeptide bands in purified PFs were evident by SDS-PAGE (not shown). PFs were com-

TABLE 1. Shape of cell body, PC, and PFs of *T. denticola*[a]

Cell structure	Shape (%)	Mean helix pitch (μm) ± SD	Mean helix diam (μm) ± SD
Cell body of strains	Irregular (>85)		
33520	Right-handed (<15)	1.19 ± 0.07	0.20 ± 0.04
35405	Right-handed (<15)	1.05 ± 0.08	0.26 ± 0.06
JR1	Right-handed	1.20 ± 0.10	0.20 ± 0.04
HL51	Right-handed	1.08 ± 0.08	0.28 ± 0.06
PC of 33520[b]	Right-handed	0.91 ± 0.09	0.21 ± 0.02
PFs of 33520[c]	Left-handed	0.78 ± 0.09	0.26 ± 0.04

[a] n = 20 for each measurement.
[b] The PC was obtained by removal of the outer membrane sheath with Triton X-100.
[c] Measurements from reference 6.

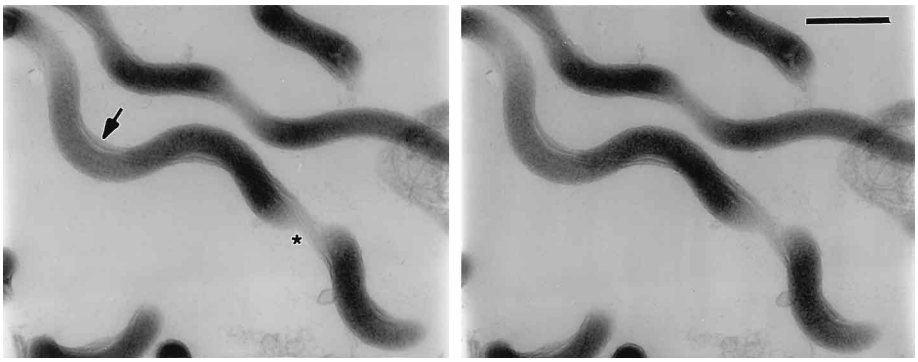

FIG. 2. High-voltage electron micrographs of a stereo pair of *T. denticola* 33520. The bottom cell has a helical region near the lower part of the figure and a planar region near the top. Note that the PFs (arrow) wrap around the body axis in the planar region and lie along the cell axis in the helical region. The asterisk identifies a lowermost sector of the cell in the helical region that was cut off during sectioning, revealing that the PFs lie on top. Bar, 0.5 μm.

prised of two major bands at 38 and 35 kDa and two minor bands at 32 and 29 kDa (42, 43). These results are similar to those reported by Cockayne et al. (9).

Two-dimensional gel electrophoresis of whole-cell lysates (Fig. 4a) indicated that although the protein composition of *T. denticola* showed some similarities to those of both *T. pallidum* and *T. phagedenis*, the overall pattern was distinctly different (compare Fig. 4a to Fig. 1 in reference 34). An analysis of

FIG. 3. Electron micrographs of cells negatively stained with uranyl acetate. (a) Wild-type *T. denticola* 33520 showing the PFs extending backward along the length of the cell; (b) mutant JR1, with short, stubby PFs. Arrows point to PFs. Bar, 0.1 μm.

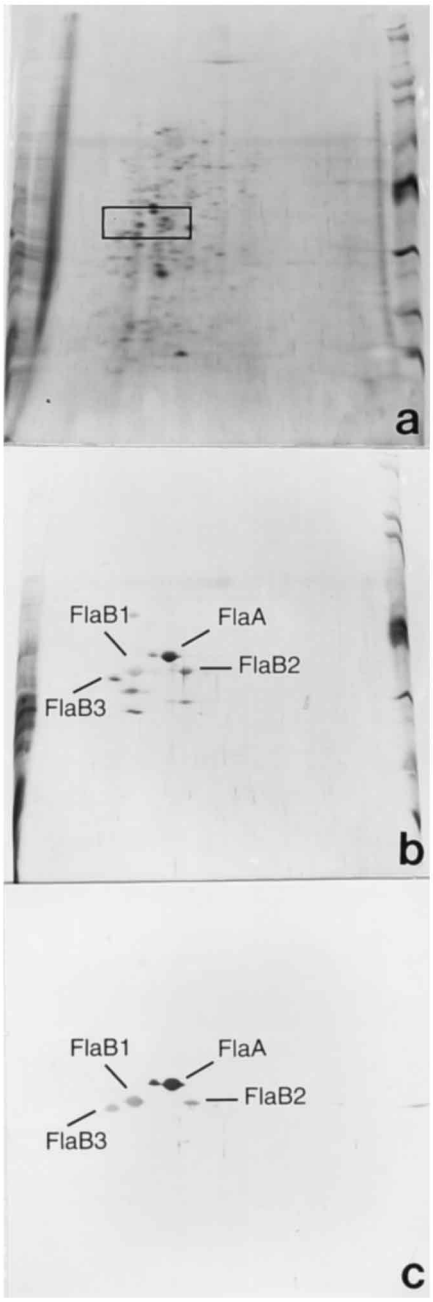

FIG. 4. (a) Distribution of proteins after two-dimensional electrophoresis of whole-cell lysates of *T. denticola* 33520. Proteins were visualized by silver staining. The FlaA and FlaB proteins are boxed. (b) Purified PFs of strain 33520 visualized by silver staining. The locations of FlaA and FlaB proteins are indicated. (c) Western blot of purified PFs reacted with FlaA antiserum followed by FlaB2 antiserum from *T. pallidum*. The proteins that reacted with specific antisera are indicated.

purified PFs by two-dimensional gel electrophoresis indicated that the 35-kDa band observed during SDS-PAGE was actually composed of two 35-kDa polypeptides and one 34-kDa polypeptide. In addition, the 32-kDa SDS-PAGE band was resolved into discrete 32- and 31-kDa polypeptide species. Other polypeptides present in the PF preparations were at 52, 38, and 29 kDa (Fig. 4b).

To analyze these polypeptides in detail, immunoblots were prepared by using antisera specific to the FlaA and FlaB2 PF proteins of *T. pallidum* (34). Only the 38-kDa protein of *T. denticola* reacted with the anti-FlaA serum in both whole-cell lysates (not shown) and purified PFs (Fig. 4c). In assays using antiserum to the FlaB2 protein, three protein species reacted: two of 35 kDa (designated FlaB1 and FlaB2) and one of 34 kDa (designated FlaB3) (Fig. 4c). These results indicate that *T. denticola* PFs have one 38-kDa FlaA protein and three FlaB proteins (two of 35 kDa and one of 34 kDa).

N-terminal amino acid sequence of PF polypeptides. The *T. denticola* FlaA and FlaB proteins were isolated by two-dimensional gel electrophoresis and analyzed by N-terminal amino acid sequencing. Each of the FlaA and FlaB proteins had a unique sequence over the first 30 amino acids (Fig. 5). *T. denticola* PF proteins most closely resembled those of *T. pallidum* and *T. phagedenis*. *T. denticola* FlaA had 67% identity with *T. pallidum* FlaA. *T. denticola* FlaB1, FlaB2, and FlaB3 had 80 to 90% identity with their *T. pallidum* and *T. phagedenis* FlaB counterparts. In contrast, the FlaB proteins of *T. denticola* had only 63 to 77% sequence identity. These results, as noted for FlaB proteins of other spirochetes (8, 35, 36), suggest that the *T. denticola* FlaB proteins are more closely related to their heterologous counterparts than they are to each other.

Western blot of PF mutants. JR1, HL51, and the revertant JR1-r were analyzed for the ability to synthesize PF proteins by Western blot analysis. Neither of the mutants reacted with the *T. pallidum* FlaA antisera as determined by SDS-PAGE and Western blot analysis, whereas the motile revertant JR1-r regained the ability to synthesize this protein in an amount similar to that of the wild-type (Fig. 6A and B, top). Using antisera to *T. pallidum* or to *T. phagedenis* FlaB proteins, no reaction was detected in JR1, and only a trace was detected in HL51 (Fig. 6A and B, bottom). Thus, Western blot analysis confirmed the evidence from electron microscopy that the mutants were deficient in PF synthesis.

DISCUSSION

Logarithmic-phase cells of *T. denticola* have both right-handed helical and irregular forms, with the latter representing the predominant morphological type. Because of the small diameter of *T. denticola*, these forms could not be distinguished by dark-field microscopy at low magnification. In contrast to other spirochete species, the morphological types observed did not readily convert from one form to another. For example, cells of *B. burgdorferi* and *Leptospiraceae* markedly change their shape when reversing direction or switching from a translational to a nontranslational form (1, 14, 15). The presence of both regular and irregular forms of *T. denticola* cells has been noted by Socransky et al. (46), and Cox reported *T. denticola* cells with a planar morphology (10). In our analysis, we failed to detect entirely planar cells. It should be noted, however, that we concentrated on logarithmic-phase cells, since cells in stationary phase appeared even more variable in shape than those that were actively growing (42).

An analysis of the PF-deficient mutants and cells stripped of their OS indicated that the irregular morphology results from an interaction of the PFs with the cell cylinder. The PF-deficient mutants JR1 and HL51 were helical. Because stripped wild-type cells were helical and were morphologically similar to both mutants, the PFs and cell cylinder are apparently held in close juxtaposition to one another by the OS. This close association evidently allows the PFs to exert tension on the cell cylinder to cause the irregular morphology.

The interaction of the PFs and the cell cylinder that leads to the irregularly shaped forms is quite complex. The cell cylinder

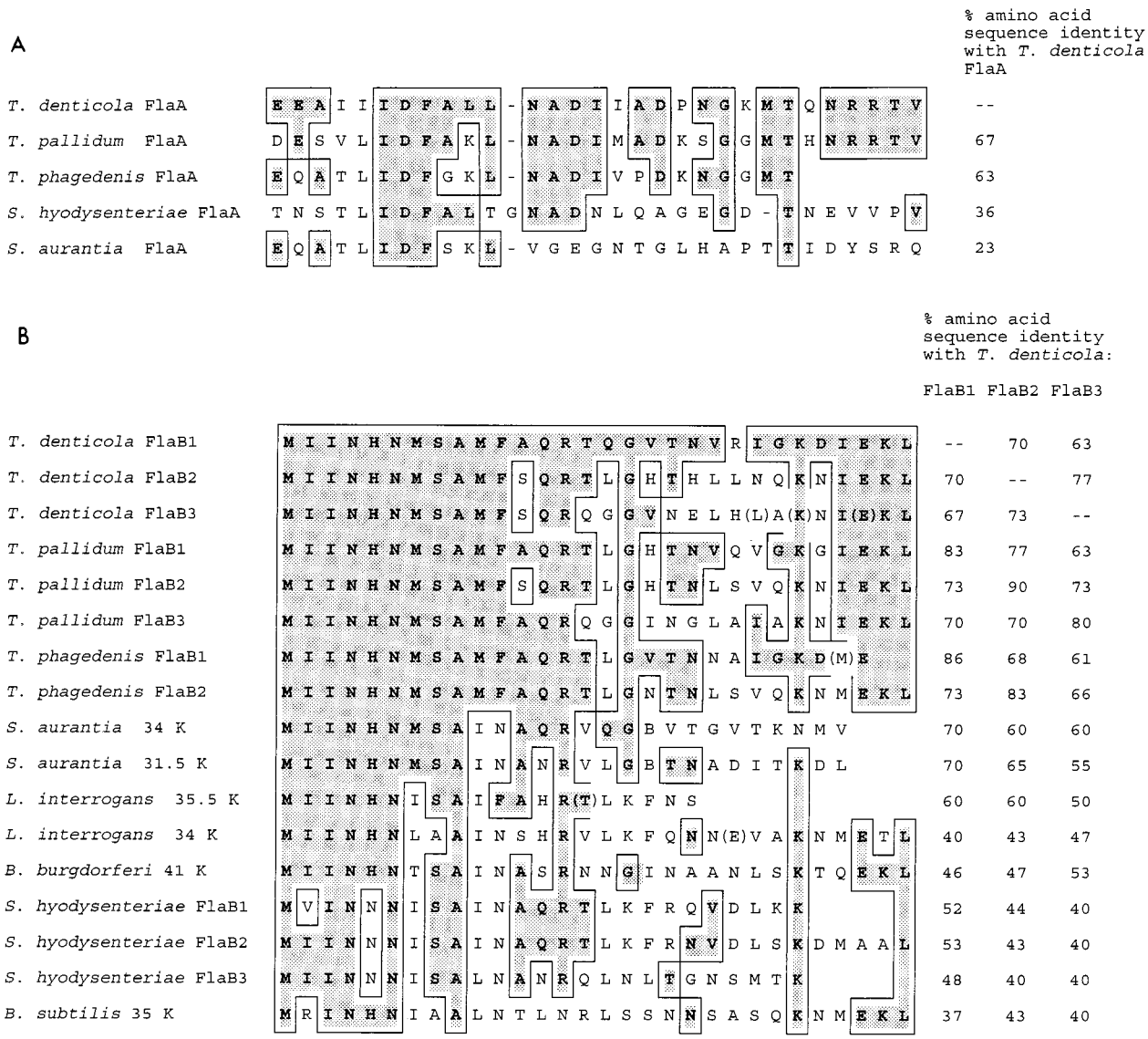

FIG. 5. N-terminal amino acid sequences of class A (A) and class B (B) proteins of *T. denticola* 33520. Sequences are compared with those of the N-terminal PF proteins of other spirochetes and with that of the flagellin of *B. subtilis*. Boxes indicate regions of amino acid identity with *T. denticola* FlaA and FlaB1, respectively. Tentative amino acid identifications are indicated by parentheses.

is right-handed, and the PFs are left-handed (Table 1). Using stereo pairs of electron micrographs, we found the pattern of winding of the PFs about the PC to be similar in many respects to those of both *B. burgdorferi* and *L. illini* (13). Specifically, as with *B. burgdorferi*, the PFs form a ridge extending along the entire length of most cells. This result is consistent with the PFs overlapping in the center of the cell, and it implies that the PFs from opposite ends of the cell interact with one another. We previously proposed that this interaction plays a central role in determining cell shape for *B. burgdorferi* (15), and we also believe this to be the case for *T. denticola*. In the planar regions of the cell, the PFs wound around the body axis in a right-handed sense, were on the axial side of the PC bends, and formed a left-handed helix along the cell axis. Similar results were found with *B. burgdorferi* (13). In contrast, the PFs tended to form a straight filament along the cell axis in those regions of the cell in which the PC had a right-handed helical or irregular form. These results are similar to those reported for *L. illini* whereby the single PF lies along the axis of the cell in the hook-shaped region (13).

The results presented indicate that phenotypic variation accounts for the two morphological forms observed. This variation could be the consequence of a variation of the PFs within

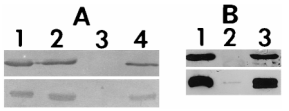

FIG. 6. (A) Western blots of PF proteins from wild-type strain 33520 and PF mutant JR1 probed with *T. pallidum* FlaA (top) and FlaB2 (bottom) antisera. Lanes: 1, purified PFs from strain 33520; 2, whole cells of strain 33520; 3, whole cells of mutant JR1; 4, whole cells of revertant JR1-r. The blot was developed with 4-chloronaphthol. (B) Western blot of wild-type strain 35405 and PF mutant HL51 probed with *T. pallidum* FlaA (top) and *T. phagedenis* FlaB (bottom) antisera. Lanes: 1, purified PFs from strain 33520; 2, whole cells of mutant HL51; 3, whole cells of strain 33405. The blot was developed by using the ECL luminol assay.

the population. Specifically, there are multiple PFs attached at each end of the cell, and their number, length, and even composition could differ from one to the other. Moreover, the way in which these PFs interact with one another and the cell cylinder during rotation could markedly influence cell morphology. Alternatively, phenotypic variation in the composition of the peptidoglycan in the cell cylinder could cause different morphological forms. For example, helical cells could have a more rigid peptidoglycan than the irregularly shaped cells and thus better resist the torsional forces exerted by the PFs, which can distort the cell body. Because partially rod-shaped cells occur in the population, as has also been observed for *T. phagedenis* (7), there is evidently variation in the structure of the cell cylinder within the population.

Short rotating protrusions were noted on JR1 cells, indicating that the proximal regions of the PFs were intact and retained functional hook-basal body complexes in this mutant. Preliminary results from two-dimensional Western blot analysis suggest that small amounts of FlaA, but not FlaB, protein may be present in whole-cell lysates of JR1 (43). These stubs could in part be comprised of FlaA proteins. Along these lines, certain flagellin mutants of *Caulobacter crescentus*, whose wild-type cells have multiple flagellin protein species, form flagellar stubs which are composed of only one antigenic type of flagellin (24).

T. denticola PFs consist of one class A protein (FlaA) and three class B PF proteins (FlaB1, FlaB2, and FlaB3). Other proteins copurified with the PFs, and it remains to be determined whether these are actually PF components. The 29-kDa protein is of the same size as a protein that copurifies with the PFs from *T. pallidum* (34). FlaA and FlaB PF proteins has been found in other spirochete genera, including *Spirochaeta* (3, 36), *Treponema* (2, 34), *Leptospira* (33, 47), *Serpulina*, and more recently *Borrelia* (8, 12, 23, 27, 35). The N-terminal amino acid sequences of the various Fla proteins indicate a close phylogenetic relationship of *T. denticola* to *T. pallidum* and to *T. phagedenis*. This close relationship of these three spirochetes is also supported by 16S ribosomal RNA gene sequence analysis (38, 39).

The *flgE* mutation in HL51 has many pleiotropic effects, including losses in PF synthesis, helical protrusions, motility, and the ability to form irregularly shaped cells. Although we do not know the site of the mutation (or mutations) in JR1, we know that HL51 resulted from insertional inactivation of the *flgE* gene. Evidently *flgE* is involved in expression of the FlaA and FlaB proteins, since no FlaA and only a trace of FlaB was detected in cell lysates of HL51. Although other explanations are possible, these results are consistent with the synthesis of PF proteins in *T. denticola* being regulated in a hierarchical manner, as is flagellar synthesis in other bacteria (31). As more motility genes are identified in *T. denticola* (16), site-directed mutagenesis studies should yield information on the nature of the regulatory mechanisms involved in PF synthesis in these organisms.

ACKNOWLEDGMENTS

We thank T. Beveridge and the Guelph Regional STEM Facility, Y. Ge, and J. Howell for technical assistance and D. Yelton for suggestions.

This research was supported by Public Health Service grants DE04645 and DE012046 to N.W.C., K11DE000257 to J.D.R., and DE09821 to H.K. In addition, K.F.B. and the HVEM facility were supported by grant RR 01219 awarded by the Biotechnology Area, National Center for Research Resources (DHHR/PHS), to support the Wadsworth Center's Biological Microscopy and Image Reconstruction Facility as a National Biotechnological Resource.

REFERENCES

1. **Berg, H. C., D. B. Bromley, and N. W. Charon.** 1978. Leptospiral motility. Symp. Soc. Gen. Microbiol. **28:**285–294.
2. **Blanco, D. R., C. I. Champion, J. N. Miller, and M. A. Lovett.** 1988. Antigenic and structural characterization of *Treponema pallidum* (Nichols strain) endoflagella. Infect. Immun. **137:**2973–2979.
3. **Brahamsha, B., and E. P. Greenberg.** 1988. A biochemical and cytological analysis of the complex periplasmic flagella from *Spirochaeta aurantia*. J. Bacteriol. **170:**4023–4042.
4. **Bromley, D. B., and N. W. Charon.** 1979. Axial filament involvement in the motility of *Leptospira interrogans*. J. Bacteriol. **137:**1406–1412.
5. **Canale-Parola, E.** 1984. The spirochetes, p. 38–70. *In* N. R. Krieg and J. G. Holt (ed.), Bergey's manual of systematic bacteriology. Williams and Wilkins, Baltimore, Md.
6. **Charon, N. W., S. F. Goldstein, S. M. Block, K. Curci, J. D. Ruby, J. A. Kreiling, and R. J. Limberger.** 1992. Morphology and dynamics of protruding spirochete periplasmic flagella. J. Bacteriol. **174:**832–840.
7. **Charon, N. W., S. F. Goldstein, K. Curci, and R. J. Limberger.** 1991. The bent-end morphology of *Treponema phagedenis* is associated with short, left-handed periplasmic flagella. J. Bacteriol. **173:**4820–4826.
8. **Charon, N. W., E. P. Greenberg, M. B. H. Koopman, and R. J. Limberger.** 1992. Spirochete chemotaxis, motility, and the structure of the spirochetal periplasmic flagella. Res. Microbiol. **143:**597–603.
9. **Cockayne, A., R. Sanger, A. Ivic, R. A. Strugnell, J. H. MacDougall, R. R. Russell, and C. W. Penn.** 1989. Antigenic and structural analysis of *Treponema denticola*. J. Gen. Microbiol. **135:**3209–3218.
10. **Cox, C. D.** 1972. Shape of *Treponema pallidum*. J. Bacteriol. **109:**943–944.
11. **Ellen, R. P., J. R. Dawson, and P. F. Yang.** 1994. *Treponema denticola* as a model for polar adhesion and cytopathogenicity of spirochetes. Trends Microbiol. **2:**114–119.
12. **Ge, Y., and N. W. Charon.** 1996. An unexpected *flgA* homolog is present and expressed in *Borrelia burgdorferi*. J. Bacteriol. **179:**552–556.
13. **Goldstein, S. F., K. F. Buttle, and N. W. Charon.** 1996. Structural analysis of *Leptospiraceae* and *Borrelia burgdorferi* by high-voltage electron microscopy. J. Bacteriol. **178:**6539–6545.
14. **Goldstein, S. F., and N. W. Charon.** 1988. The motility of the spirochete *Leptospira*. Cell Motil. Cytoskel. **9:**101–110.
15. **Goldstein, S. F., N. W. Charon, and J. A. Kreiling.** 1994. *Borrelia burgdorferi* swims with a planar waveform similar to that of eukaryotic flagella. Proc. Natl. Acad. Sci. USA **91:**3433–3437.
16. **Heinzerling, H. F., J. E. Penders, and R. A. Burne.** 1995. Identification of a *fliG* homologue in *Treponema denticola*. Gene **161:**69–73.
17. **Holt, S. C.** 1978. Anatomy and chemistry of spirochetes. Microbiol. Rev. **42:**114–160.
18. **Hovind Hougen, K.** 1976. Determination by means of electron microscopy of morphological criteria of value for classification of some spirochetes, in particular treponemes. Acta. Pathol. Microbiol. Scand. Sect. B Suppl. **255:** 1–41.
19. **Hovind Hougen, K.** 1979. *Leptospiraceae*: a new family to include *Leptospira* Noguchi 1917 and *Leptospira* gen. nov. Int. J. Syst. Bacteriol. **29:**245–251.
20. **Hovind Hougen, K.** 1984. Ultrastructure of spirochetes isolated from *Ixodes ricinus* and *Ixodes dammini*. Yale J. Biol. Med. **57:**543–548.
21. **Hyat, M. A.** 1986. Basic techniques for transmission electron microscopy. Academic Press, Inc., Orlando, Fla.
22. **Klitorinos, A., P. Noble, R. Siboo, and E. C. S. Chan.** 1993. Viscosity-dependent locomotion of oral spirochetes. Oral Microbiol. Immunol. **8:**242–244.
23. **Koopman, M. B. H., E. Baats, C. J. A. H. V. van Vorstenbosch, B. A. M. van der Ziejst, and J. G. Kusters.** 1992. The periplasmic flagella of *Serpulina* (*Treponema*) *hyodysenteriae* are composed of two sheath proteins and three core proteins. J. Gen. Microbiol. **138:**2697–2706.
24. **Koyasu, S., M. Asada, A. Fukuda, and Y. Okada.** 1981. Sequential polymersization of flagellin A and flagellin B into *Caulobacter* flagella. J. Mol. Biol. **153:**471–475.
25. **Leschine, S. B., and E. Canale-Parola.** 1980. Rifampin as a selective agent for isolation of oral spirochetes. J. Clin. Microbiol. **12:**792–795.
26. **Li, H., J. Ruby, N. Charon, and H. Kuramitsu.** 1996. Gene inactivation in the oral spirochete *Treponema denticola*: construction of a *flgE* mutant. J. Bacteriol. **178:**3664–3667.
27. **Li, Z., F. Dumas, D. Dubreuil, and M. Jacques.** 1993. A species-specific periplasmic flagellar protein of *Serpulina* (*Treponema*) *hyodysenteriae*. J. Bacteriol. **175:**8000–8007.
28. **Limberger, R. J., and N. W. Charon.** 1986. *Treponema phagedenis* has at least two proteins residing together on its periplasmic flagella. J. Bacteriol. **166:** 105–112.
29. **Limberger, R. J., and N. W. Charon.** 1986. Antiserum to the 33,000-dalton periplasmic-flagellum protein of *Treponema phagedenis* reacts with other treponemes and *Spirochaeta aurantia*. J. Bacteriol. **168:**1030–1032.
30. **Loesche, W. J., and B. E. Laughon.** 1982. Role of spirochetes in periodontal diseases, p. 67–75. *In* R. J. Genco and S. A. Mergenhagen (ed.), Host-parasite interactions in periodontal diseases. American Society for Microbiology, Washington, D.C.

31. **Macnab, R. M.** 1996. Flagella and motility, p. 123–145. *In* F. C. Neidhardt, R. Curtiss III, J. L. Ingraham, E. C. C. Lin, K. B. Low, B. Magasanik, W. S. Reznikoff, M. Riley, M. Schaechter, and H. E. Umbarger (ed.), *Escherichia coli* and *Salmonella*: cellular and molecular biology. ASM Press, Washington, D.C.
32. **Matsudaira, P.** 1987. Sequence from picomole quantities of proteins electroblotted onto polyvinylidene difluoride membranes. J. Biol. Chem. **262:** 10035–10038.
33. **Mitchison, M., J. I. Rood, S. Faine, and B. Adler.** 1991. Molecular analysis of a *Leptospira borgpetersenii* gene encoding an endoflagellar subunit protein. J. Gen. Microbiol. **137:**1529–1536.
34. **Norris, S. J., N. W. Charon, R. G. Cook, M. D. Fuentes, and R. J. Limberger.** 1988. Antigenic relatedness and N-terminal sequence homology define two classes of major periplasmic flagellar proteins of *Treponema pallidum* subsp. *pallidum* and *Treponema phagedenis*. J. Bacteriol. **170:**4072–4082.
35. **Norris, S. J., and *Treponema pallidum* Polypeptide Research Group.** 1993. Polypeptides of *Treponema pallidum*: progress toward understanding their structural, function, and immunologic roles. Microbiol. Rev. **57:**750–779.
36. **Parales, J. J., and E. P. Greenberg.** 1991. N-terminal amino acid sequences and amino acid compositions of the *Spirochaeta aurantia* flagellar filament polypeptides. J. Bacteriol. **173:**1357–1359.
37. **Paster, B. J., and E. Canale-Parola.** 1980. Involvement of periplasmic fibrils in motility of spirochetes. J. Bacteriol. **141:**359–364.
38. **Paster, B. J., F. E. Dewhirst, S. M. Cooke, V. Fussing, L. K. Poulsen, and J. A. Breznak.** 1996. Phylogeny of not-yet-cultured spirochetes from termite guts. Appl. Environ. Microbiol. **62:**347–352.
39. **Paster, B. J., F. E. Dewhirst, W. G. Weisburg, L. A. Tordoff, G. J. Fraser, R. B. Hespell, T. B. Stanton, L. Zablen, L. Mandelco, and C. R. Woese.** 1991. Phylogenetic analysis of the spirochetes. J. Bacteriol. **173:**6101–6109.
40. **Pietrantonoio, F., P. B. Noble, R. Amsel, and E. C. S. Chan.** 1988. Locomotory characteristics of *Treponema denticola*. Can. J. Microbiol. **34:**748–752.
41. **Rosey, E., M. J. Kennedy, D. K. Petrella, R. G. Ulrich, and R. J. J. Yancey.** 1995. Inactivation of *Serpulina hyodysenteriae flaA1* and *flaB1* periplasmic flagellar genes by electroporation-mediated allelic exchange. J. Bacteriol. **177:**5959–5970.
42. **Ruby, J. D., and N. W. Charon.** 1996. Unpublished data.
43. **Ruby, J. D.** 1995. *Treponema denticola* periplasmic flagella and motility. Ph.D. dissertation. West Virginia University, Morgantown, W. Va.
44. **Sadziene, A., D. D. Thomas, V. G. Bundoc, S. C. Holt, and A. G. Barbour.** 1991. A flagella-less mutant of *Borrelia burgdorferi*. Structural, molecular, and in vitro characterization. J. Clin. Invest. **88:**82–92.
45. **Simonson, L. G., C. H. Goodman, J. J. Bial, and H. E. Morton.** 1988. Quantitative relationship of *Treponema denticola* to severity of periodontal disease. Infect. Immun. **56:**726–728.
46. **Socransky, S., M. Listgarten, C. Hubersak, J. Cotmare, and A. Clark.** 1969. Morphological and biochemical differentiation of three types of small oral spirochetes. J. Bacteriol. **98:**878–882.
47. **Trueba, G. A., C. A. Bolin, and R. L. Zuerner.** 1992. Characterization of the periplasmic flagellum proteins of *Leptospira interrogans*. J. Bacteriol. **174:** 4761–4768.
48. **Woese, C. R.** 1987. Bacterial evolution. Microbiol. Rev. **51:**221–271.
49. **Yelton, D. B., R. J. Limberger, K. Curci, F. Malinosky-Rummell, L. Slivienski, L. M. Schouls, J. D. A. van Embden, and N. W. Charon.** 1991. *Treponema phagedenis* encodes and expresses homologs of the *Treponema pallidum* TmpA and TmpA proteins. Infect. Immun. **59:**3685–3693.